Int. J. Solids Structures Vol. 26, No. 12, pp. 1371–1386, 1990
Printed in Great Britain.

0020–7683/90 \$3.00+ .00
Pergamon Press plc

BUCKLING OF CRACKED COMPOSITE COLUMNS

KAMYAR NIKPOUR
Mechanical Engineering Department, Crothers Engineering Hall, Room 210,
South Dakota State University, Brookings, SD 57007, U.S.A.

(*Received* 28 *March* 1989; *in revised form* 2 *November* 1989)

Abstract—A crack in a structural element introduces a significant local flexibility which enhances the instability. Buckling of an edge-notched beam is studied for isotropic and anisotropic composites. The local compliance due to the presence of cracks in an anisotropic medium is formulated as a function of the crack-tip stress intensity factors and the elastic constants of the material. The general integration of the non-linear differential equations expressing the buckling model of an eccentrically loaded composite beam is derived for two different types of hinged supports; namely freely approaching and fixed span. The effect of reducing rigidity on the load-carrying capacity and the post-buckling behavior of the beam is discussed and exemplary numerical solutions are provided. The study indicates that the instability increases with the beam slenderness and the crack length. In addition, the material anisotropy conspicuously reduces the load-carrying capacity of an externally cracked member.

NOMENCLATURE

A_{ij}	material elastic constants
$a(\bar{a})$	(dimensionless) crack length
B	beam thickness
C	apparent compliance factor
C_1, C_2	anisotropic perturbation factors
D	maximum deflection
d_1	compression factor
d_2	bending factor
E_1, E_2	elliptical integrals of the first and second kind, respectively
E_F, E_T	modulus of elasticity in fiber and transverse directions
$e(\bar{e})$	(dimensionless) eccentricity
G	strain energy release function
G_{FT}	orthotropic shear modulus
I	moment of inertia
K_I, K_{II}	first and second mode stress intensity factors
L	beam length
$M(\bar{M})$	(virtual) bending moment
P	compressive load
P_{cr}	nominal critical load
p	parameter of the elliptical integrals
$S(\bar{S})$	(dimensionless) approach
$U(U_0)$	(initial) strain energy
$W(\bar{W})$	(dimensionless) specimen width
$X(\bar{X})$	(dimensionless) coordinate along beam axis
$Y(\bar{Y})$	dimensionless deflection
Y_1, Y_2	correction factors in K_I and K_{II} expressions

Greek symbols

α	$\pi\bar{a}$
β	$(1/6)(Y_1/Y_2)$
$\Delta(\bar{\Delta})$	(dimensionless) central deflection
ϕ, ϕ_0, ϕ_m	phase angles in elliptical integrals
ν_{FF}	Poisson ratio (orthotropic plane)
ν_{TT}	Poisson ratio (isotropic plane)
θ_c	relative angular rotation of the cracked element
η	anisotropic quotient
λ	dimensionless load
μ_1, μ_2	complex roots of the characteristic equation of composites.

1. INTRODUCTION

In recent years, the use of anisotropic reinforced composites, where weight is a primary concern, has increased substantially in the fields of mechanical and civil engineering. Because

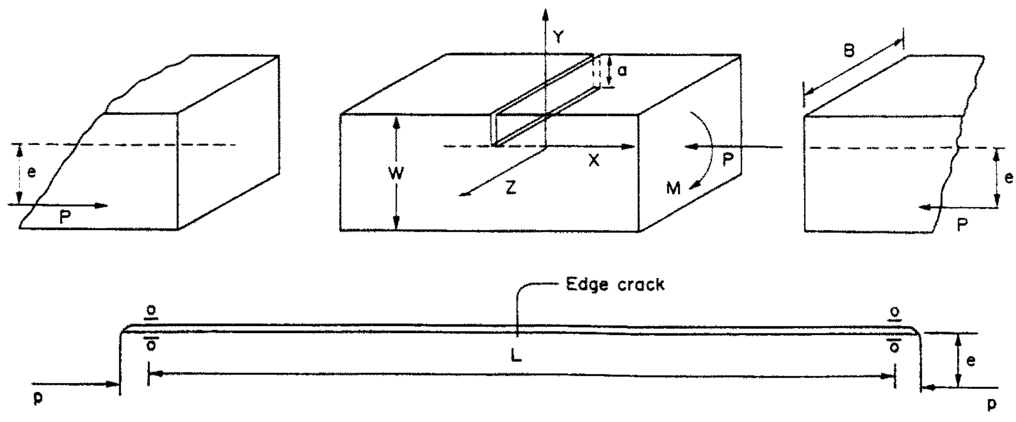

Fig. 1. Geometry of a rectangular beam with a single edge crack.

of this the problem of the structural integrity and failure processes of these composites has been investigated extensively. It is clear that the existence of intrinsic flaws or artificial stress-concentrators cannot be precluded and the detrimental effects of these phenomena are more conspicuous for fibrous composites. In principle, cracks are the cause of incipient failure, if overloading or fatigue renders their unstable propagation. A brief survey on the fracture mechanics of unidirectional composites is given in a recent paper by Nikpour *et al.* (1990). However, prior to fracture, the crack can induce severe local flexibility which contributes to the premature buckling of the component under compressive forces.

The instability of isotropic cracked columns has been reported firstly by Liebowitz and Claus (1968) and Liebowitz *et al.* (1967). They observed that the local compliance due to the presence of cracks enhances the lateral deflection of a column under eccentric loads. Later, theoretical formulation of the problem was given by Okamura *et al.* (1969), who employed the principles of fracture mechanics on the deformation of cracked columns. Also, the post-buckling of isotropic columns with an edge flaw was investigated by Anifantis and Dimarogonas (1983) using the well known Paris equation for the deflection of cracked bodies. Rice and Levy (1972) reported the coupling between tensile and bending compliances of cracked beams, and Anifantis and Dimarogonas (1984) gave the complete 5×5 compliance matrix, reflecting the possible coupling of the shear and normal forces.

The local compliance matrix for anisotropic materials was introduced by Nikpour and Dimarogonas (1988), where it has been shown that the interlocking deflection modes are enhanced as a function of the degree of anisotropy in composites. The effect of cracks upon vibrational response of isotropic materials has been studied by many investigators (Papadopoulos and Dimarogonas, 1987, 1988; Chondros and Dimarogonas, 1980) and presently, it is being investigated for unidirectional fibrous composites by the author (Nikpour, 1990).

This paper is aimed at a characterization of the buckling nature of fibrous materials due to local compliances.

2. LOCAL FLEXIBILITY

The weakening effect of a crack can be best explained in terms of the local flexibility coefficients. For an anisotropic component these coefficient are to be defined in terms of the material compliance factors as well as the geometry of the crack dimension and position. Figure 1 shows a single edge-notched prismatic bar of length L under combined bending and compressive forces. The width and thickness are denoted by W and B, respectively. The plane of the crack is taken at the central section of the beam, perpendicular to its longitudinal axis and with a uniform depth, a, through the thickness. The material is assumed to be orthotropic fiber-reinforced composites (such as wood and osseous structures) whose principal axes coincide with the geometrical directions of the beam. Therefore, the crack surface is either parallel or perpendicular to the filamentary direction. The simplicity of the crack configuration facilitates the mathematical modeling of the problem, though the buckling behavior of more complicated structures can be phenomenologically understood from the results presented.

To define the crack compliance, an infinitesimal element of the beam in the vicinity of the cracked plane is isolated and is acted upon by a normal compressive load P and a bending moment M. The moment is assumed to be parallel to the crack front such that on the simple beam theory, the diminutive effect of shear stresses on the lateral deflection can be neglected. However, the coupling of the shear and bending components of the local compliance is a characteristic feature of anisotropic materials (Nikpour and Dimarogonas, 1988) which aggravates the structural stability. Presently, shear forces are not considered and the pure bending is merely caused by the eccentricity of the applied load with reference to the neutral axis of the deflected beam. At the central cross-section bending is maximum and equal to

$$M = (D+e)P, \tag{1}$$

where e and D denote the initial eccentricity and the central deflection of the beam, respectively.

Let θ_c be the relative angular rotation of the end faces of the cracked element and U be the strain energy restored in it. From Castigliano's theorem, we have

$$\theta_c = \left[\frac{\partial}{\partial \bar{M}} U(P, \bar{M})\right]_{\bar{M} \to 0}, \tag{2}$$

where $\bar{M}$ is the virtual moment acting in the direction of rotation and will be set to zero after carrying out the derivation. According to Paris' law (Tada *et al.*, 1973), the change in the strain energy due to the presence of a crack of length a, is related to the strain energy release rate, G, by

$$\Delta U = B \int_0^a G(a)\, \mathrm{d}a. \tag{3}$$

Let U_0 be the strain energy in the absence of crack, so that the total strain energy will be

$$U = U_0 + \Delta U. \tag{4}$$

Since the θ_c arises from the crack singularity at the middle section and U_0 gives no contribution to it, on substituting eqns (4) and (3) into eqn (2), we can write:

$$\theta_c = B \lim_{\bar{M} \to 0} \int_0^a \frac{\partial}{\partial \bar{M}} G(P, \bar{M})\, \mathrm{d}a. \tag{5}$$

In the absence of torsion, the strain energy release rate can be defined in terms of the opening and inplane sliding stress intensity factors K_I and K_{II}. For an anisotropic material this relationship is in the form (Nikpour and Dimarogonas, 1988):

$$G = -\frac{A_{22}}{2} \operatorname{Im}\left(\frac{\mu_1+\mu_2}{\mu_1\mu_2}\right) K_I^2 + \frac{A_{11}}{2} \operatorname{Im}(\mu_1+\mu_2) K_{II}^2 + A_{11} \operatorname{Im}(\mu_1\mu_2) K_I K_{II}. \tag{6}$$

If the material is transversely isotropic with the principal axes oriented perpendicular (x-direction) and parallel to the crack front (y-direction), the normal stresses give rise to the opening mode only, and we have $K_{II} = 0$.

Under plane strain conditions, the elastic constants A_{11}, A_{12}, A_{22} and A_{66} can be expressed in terms of the commonly known filamentary and transverse moduli (E_F and E_T, respectively), orthotropic shear modulus (G_{FT}) and Poisson ratios (ν_{FT} and ν_{TT}), where the latter is measured in an isotropic plane perpendicular to the filaments and the former is the ratio of transverse to filamentary displacements, when the stress is applied in the filamentary direction. These are

$$A_{11} = \frac{1}{E_F}\left(1 - \frac{E_T}{E_F}\nu_{FT}^2\right), \quad A_{22} = \frac{1}{E_T}(1-\nu_{TT}^2)$$

$$A_{12} = -\frac{\nu_{FT}}{E_F}(1+\nu_{TT}), \quad A_{66} = \frac{1}{G_{FT}}. \tag{7}$$

The complex numbers μ_1 and μ_2 in eqn (6) are the two nonconjugate roots of the characteristic equation (Sih *et al.*, 1965):

$$A_{11}\mu^4 + (2A_{12}+A_{66})\mu^2 + A_{22} = 0. \tag{8}$$

Substituting the roots of the above equation into eqn (5) yields:

$$\theta_c = B\left[\int_0^a \frac{\partial}{\partial M}\left(-\frac{A_{22}}{2}\,\mathrm{Im}\,\frac{\mu_1+\mu_2}{\mu_1\mu_2}\right)K_I^2\,\mathrm{d}a\right] \tag{9}$$

Introducing the anisotropic number

$$\eta = -\frac{A_{22}}{2A_{11}}\,\mathrm{Im}\left(\frac{\mu_1+\mu_2}{\mu_1\mu_2}\right) = \left(\frac{A_{22}}{A_{11}}\right)^{1/2}\cdot\left[\left(\frac{A_{22}}{A_{11}}\right)^{1/2} + \frac{2A_{12}+A_{66}}{2A_{11}}\right]^{1/2}$$

$$= \frac{1}{2}\frac{E_F}{E_T}\frac{1-\nu_{TT}^2}{1-(E_T/E_F)\nu_{FT}^2}\left\{\frac{E_F}{2G_{FT}} - \nu_{FT}(1+\nu_{TT}) + \left[\left(1-\nu_{TT}^2\right)\left(\frac{E_F}{E_T}-\nu_{FT}^2\right)\right]^{1/2}\right\}^{1/2} \tag{10}$$

into eqn (9), we have:

$$\theta_c = \lim_{\bar{M}\to 0}\left(2B\frac{\eta}{E_F}\int_0^a K_I\frac{\partial K_I}{\partial \bar{M}}\,\mathrm{d}a\right). \tag{11}$$

The stress intensity factor, K_I in eqn (6) for the eccentric compression and the virtual bending of the edge-notched composite beam can be expressed as (Nikpour and Dimarogonas, 1988):

$$K_I = \frac{P}{WB}\sqrt{\pi a}\left[\frac{6(e+D)}{W}Y_2 - Y_1\right] + \frac{\bar{M}}{WB}\sqrt{\pi a}\left(\frac{6}{W}Y_2\right) \tag{12}$$

The correction factors Y_1 and Y_2 arise from the lack of symmetry and the deformation at the free edges of the beam as compared with an infinite plate containing a central crack. Generally, these factors are non-dimensional functions of the crack–width ratio ($\bar{a} = a/W$) and the anisotropic constants of material which may be expressed in terms of the roots of the characteristic eqn (7). In many cases, however, the numerical analysis of highly anisotropic materials demonstrates a very weak correlation between the materials anisotropic constants and Y-factors. Denoting these anisotropic perturbations by $C_1(\bar{a})$ and $C_2(\bar{a})$, the Y-factors for the isotropic case can be readjusted to give (Tada *et al.*, 1973):

† Under plane stress conditions, the constants are reduced to $A_{11} = 1/E_F$, $A_{22} = 1/E_T$, $A_{12} = -\nu_{FT}/E_F$ and $A_{66} = 1/G_{FT}$.

$$Y_1 = \left(\frac{\sqrt{\tan\alpha/\alpha}}{\cos\alpha}\right)[0.752+2.02\bar{a}+0.37(1-\sin\alpha)^3]C_1(\bar{a})$$

$$Y_2 = \left(\frac{\sqrt{\tan\alpha/\alpha}}{\cos\alpha}\right)[0.923+0.19\bar{a}(1-\sin\alpha)^4]C_2(\bar{a}) \tag{13}$$

where $\alpha = \pi\bar{a}$ and factors C_1 and C_2 are functions of the crack length and material elastic constants. To cite an example the numerical data given by Delale *et al.* (1979) for a boron–epoxy composite (see the Appendix for the elastic constants) are interpolated into polynomial forms of the third degree as:

$$C_1 = 0.928+0.267\bar{a}-0.524\bar{a}^2+0.264\bar{a}^3 \text{ (error} < 0.004)$$

$$C_2 = 0.928+0.254\bar{a}-0.545\bar{a}^2+0.294\bar{a}^3 \text{ (error} < 0.008), \tag{14}$$

which demonstrates a maximum range of variation of less than 4%. Similar calculations for a grade of glass fiber-reinforced composite with 20% fiber volume fraction (see the Appendix) indicate that the required correction to the Y-factors is almost one-third of that introduced for the boron–epoxy composite as given by eqn (14).

Substituting the stress intensity values from eqns (12)–(14) into eqn (9), the slope of the cracked column at its central cross-section becomes:

$$Y' = \tfrac{1}{2}\theta_c = \pi^2\lambda^2\bar{W}^2[d_2\bar{\Delta}-(d_1/6)], \tag{15}$$

where $\bar{\Delta}$ is the dimensionless central deflection of the beam given by:

$$\bar{\Delta} = \frac{e+D}{W} \tag{16}$$

and $\bar{W} = W/L$. The parameter λ is the dimensionless load as compared to the nominal buckling load of an uncracked column, that is

$$\lambda^2 = \frac{P}{P_{cr}}, \tag{17}$$

in which P_{cr} for a simply supported beam is defined as usual by:

$$P_{cr} = \frac{\pi^2 E_F B W^3}{12L^2}. \tag{18}$$

The flexibility factors d_1 and d_2 are evaluated from the following integrals:

$$d_2 = 3\pi\eta\int_0^{\bar{a}} \bar{a}Y_2^2\,\mathrm{d}a$$

$$d_1 = 3\pi\eta\int_0^{\bar{a}} \bar{a}Y_1Y_2\,\mathrm{d}a. \tag{19}$$

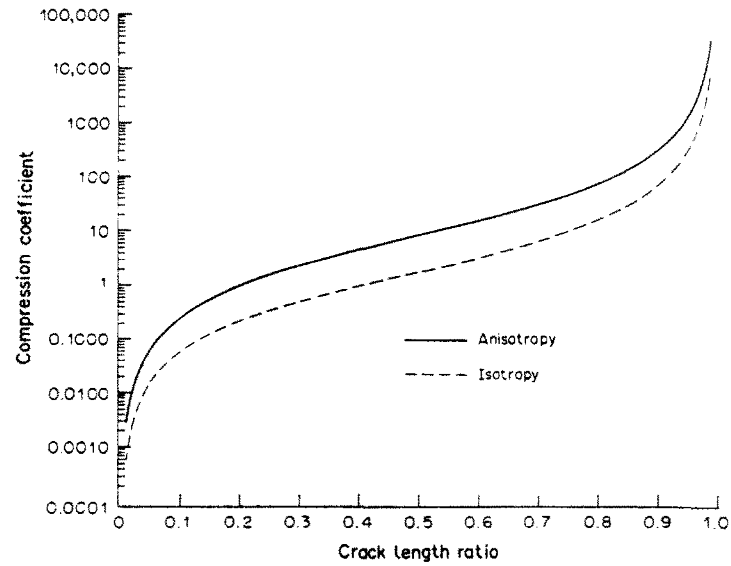

Fig. 2. Bending coefficient (d_2) as a function of crack length.

The plots of d_1 and d_2 factors versus the crack depth are shown in Figs 2 and 3. It can be seen that the local flexibility factor of the composite beam is markedly higher as compared to that of isotropic materials. On substituting d_1 and d_2 from eqns (19) into eqn (15) the apparent compliance can be designated as a function of the beam central deflection according to the following formula:

$$C = d_2\bar{\Delta} - \tfrac{1}{6}d_1 \tag{20}$$

The variation of this apparent compliance versus the crack length and the beam deflection for a grade of epoxy–boron composite is shown in Fig. 4. Clearly, the compliance is a linear function of the deflection and for medium crack lengths ($0.1 < \bar{a} < 0.9$) as long as the beam deformation is sufficiently large, it almost increases linearly with the crack size. It must be noted that the crack affects the beam flexibility only if the tensile stress caused

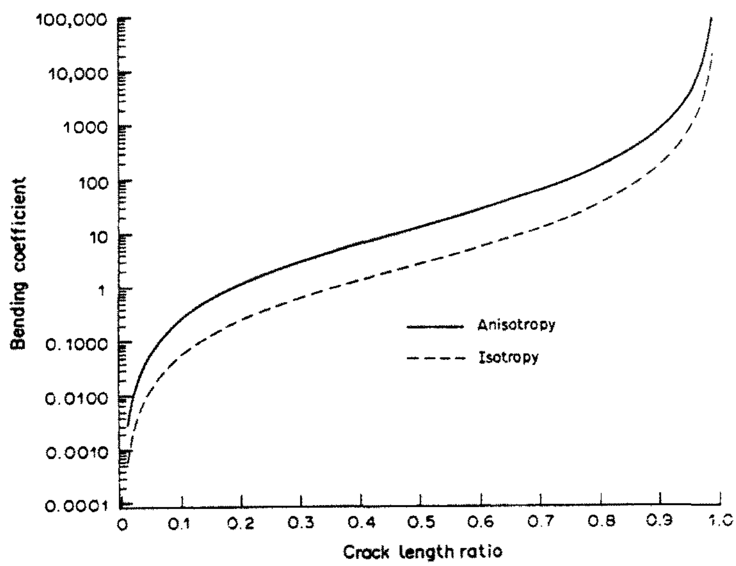

Fig. 3. Compression coefficient (d_1) as a function of crack length.

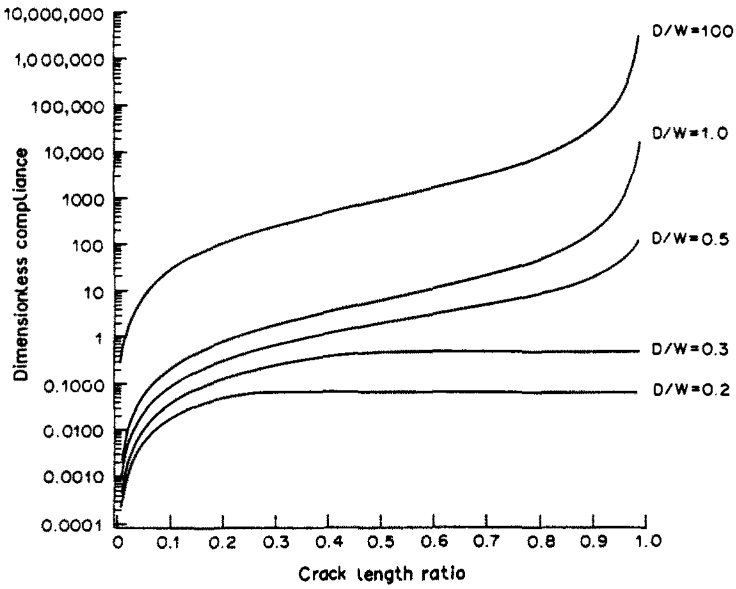

Fig. 4. Variation of the apparent compliance factor (C) with crack length ratio and dimensionless deflection (D/W).

by the bending exceeds the compressive stress due to the direct load. This requires that $K > 0$, which leads to:

$$\bar{\Delta} > \beta \tag{21}$$

where

$$\beta = \frac{1}{6}\frac{Y_1}{Y_2}.$$

Figure 5 demonstrates the variation of β as a function of the crack depth for both isotropic and anisotropic materials.

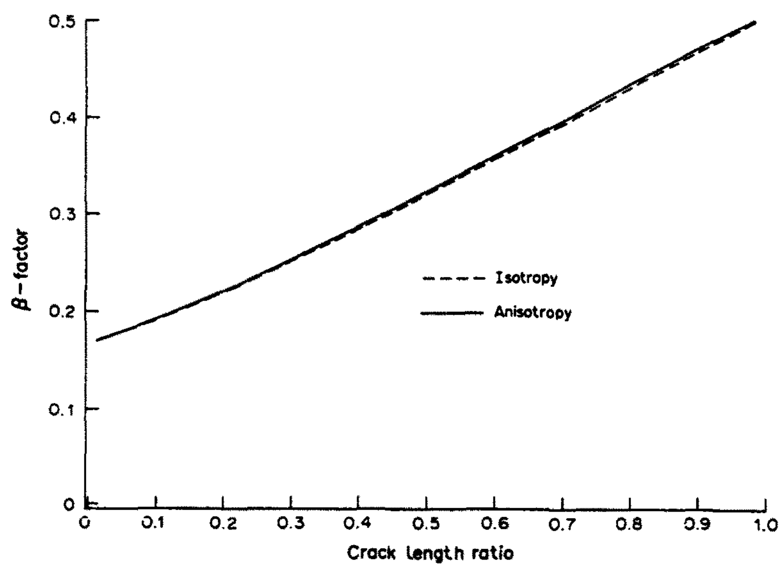

Fig. 5. Variation of β factor for isotropic and anisotropic beams.

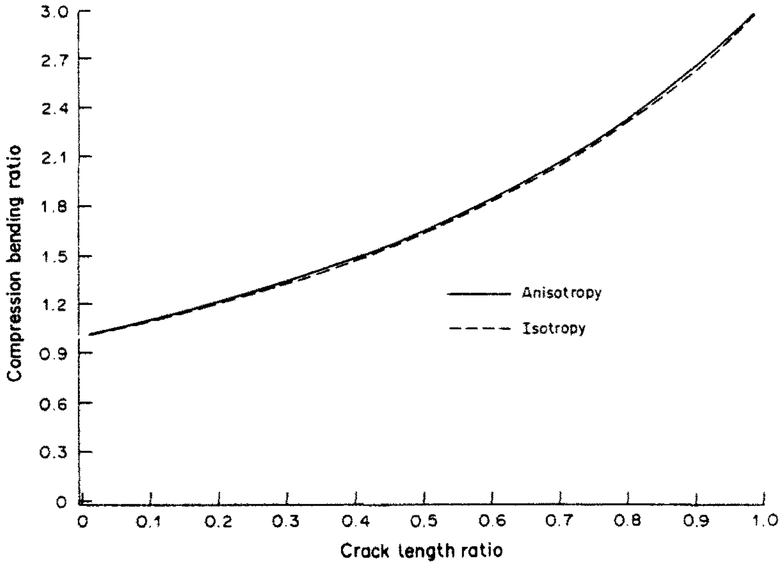

Fig. 6. d_2/d_1 versus $\bar{a}$.

3. THE NOMINAL BUCKLING LOAD

The small deflection of a prismatic cracked column subjected to an eccentric load P is characterized by:

$$E_F I \frac{d^2y}{dx^2} = -P(y+e) \tag{22}$$

where $E_F I$ is the flexural rigidity of the uncracked composite column along the fibers. The general solution of eqn (21) is:

$$y = A \sin \frac{\pi \lambda x}{L} + B \cos \frac{\pi \lambda x}{L} - e, \tag{23}$$

where the dimensionless load λ is given by eqns (17) and (18). Assuming that the beam is simply supported in both ends, then the end conditions yield $B = e$. The discontinuity in the slope of the central cross-section which arises from the local flexibility is already defined [eqn(15)], thus:

$$\frac{dy}{dx} = \pi^2 \lambda \bar{W}^2 C \quad \text{at} \quad x = L/2, \tag{24}$$

by which the constant A is evaluated to be:

$$\left(\frac{A}{L}\right) = \pi \lambda \bar{W}^2 C \sec \frac{\pi \lambda}{2} + \bar{e} \tan \frac{\pi \lambda}{2}. \tag{25}$$

On substituting eqn (25) into the general solution [eqn (23)], the maximum deflection is evaluated to be:

$$\bar{\Delta} = \left(\bar{e} - \frac{d_1 \bar{W} \pi \lambda}{6} \sin \frac{\pi \lambda}{2}\right) \Big/ \left(\cos \frac{\pi \lambda}{2} - d_2 \bar{W} \pi \lambda \sin \frac{\pi \lambda}{2}\right) \tag{26}$$

where $\bar{e} = e/W$. This may reduce to the Okamura's approximate solution if $d_2 = d_1$, which is only true for very small values of the crack length. The variation of d_1/d_2 versus $\bar{a}$ is shown in Fig. 6.

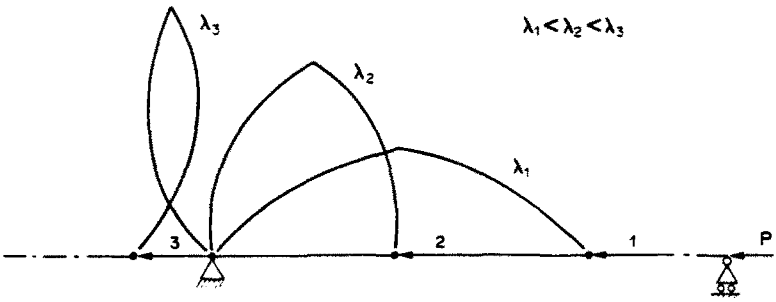

Fig. 7. Geometry of the deflected crack beam.

The load-carrying capacity of the beam is defined at the instant where the deflection approaches infinity, that is:

$$\cot \pi\lambda/2 = \pi\lambda d_2 \bar{W}, \tag{27}$$

which indicates that λ is independent of $\bar{e}$. This is of course, true if the inequality (21) is satisfied and the crack-tip surfaces bear tensile traction. However, at the instability point while D theoretically approaches infinity the crack opening requirement will be attained at a certain level of the column deformation, regardless of the size of the initial crack. For small values of d_2 (that is for relatively shallow cracks), eqn (27) reduces to:

$$\lambda = 1-2\bar{W}d_2 \simeq 1-10.2\eta\frac{a^2}{WL}, \tag{28}$$

which indicates that the load capacity decreases with the square of the crack length. The anisotropic parameter η is determined as a function of the composite elastic properties, using eqn (10). For example, in the case of the boron–epoxy composite η assumes a value of 5.46 in the filamentary direction and 1.004 in the transverse direction.

4. POST-BUCKLING BEHAVIOR

The post-buckling phenomenon is governed by the following second-order non-linear differential equation:

$$\frac{\bar{Y}''}{(1+\bar{Y}'^2)^{3/2}} \pm \pi^2\lambda^2\bar{Y} = 0, \tag{29}$$

where

$$\bar{Y} = \frac{e+y}{L},\quad \bar{X} = \frac{x}{L},\quad \bar{Y}' = \frac{\mathrm{d}\bar{Y}}{\mathrm{d}\bar{X}} = y' \quad \text{and} \quad \bar{Y}'' = \frac{\mathrm{d}^2\bar{Y}}{\mathrm{d}\bar{X}^2}$$

are the dimensionless coordinates and their derivatives. The plus or minus signs in the above equation denote positive (upward) or negative (downward) curvatures of the deflected beam, respectively. Initially, the beam deflects positively; however, at relatively high values of λ, for beyond the buckling point, the elastic line assumes alternately upward and downward curvatures (Fig. 7). Integrating the differential eqn (29), yields:

$$(1+\bar{Y}'^2)^{1/2}-(1+\bar{Y}'_0)^{-1/2} = \pm(\pi^2/2)\lambda^2(\bar{Y}^2-\bar{e}^2\bar{W}^2) \tag{30}$$

where $Y'_0 = y'_0$ is the slope at the end supports. Since the beam is cracked at its mid-cross-section, there will be a discontinuity in the slope given by eqn (15). At this point, the

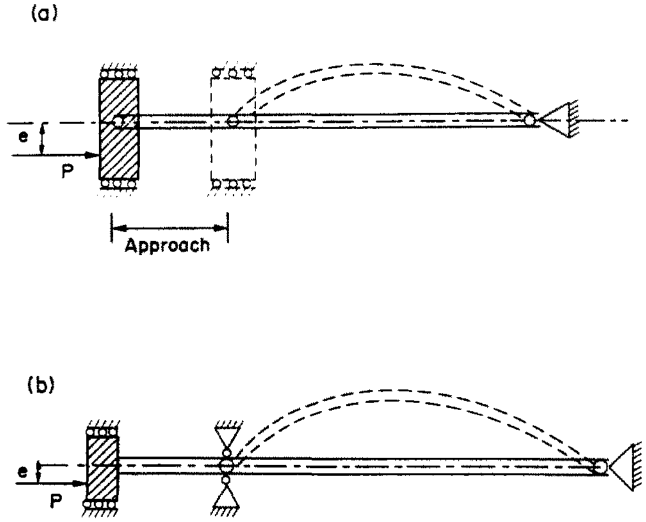

Fig. 8. Supports geometry and constraints: (a) hinged–roller, supports are free to approach each other; (b) hinged–fixed, the approach is restrained but the endless beam is free to slide over the supports.

dimensionless deflection will be as defined by eqn (16). Accordingly, the initial slope of the beam can be expressed as

$$y_0' = \pm\left\{\left[1-\frac{\pi^2\lambda^2\bar{W}^2}{2}(\Delta'^2-\bar{e}^2)\right]^{-2}+1\right\}^{1/2} \tag{31}$$

where

$$\bar{\Delta}'^2 = \bar{\Delta}^2+\frac{2}{\pi^2\lambda^2\bar{W}^2}[1-(\pi^4\lambda^4\bar{W}^4C^2+1)^{-1/2}]. \tag{32}$$

While the slope at the left-hand support and the curvature of the deflected beam are positive, the load factor, λ is limited by the following inequality to assure a real value for $\bar{Y}'$:

$$\pi^2(\bar{\Delta}'^2-\bar{e})^2\lambda^2 < 2. \tag{33}$$

At higher loads the initial curvature becomes negative and λ remains in the following range:

$$2 < \pi^2\lambda^2\bar{W}^2(\bar{\Delta}'^2-\bar{e}^2) < 4. \tag{34}$$

Referring to Fig. 8 two types of hinged supports are distinguished: (a) the roller type in which the beam is clamped between the support faces, while the supports approach each other, and (b) the fixed type in which the endless beam slides between the fixed span supports. In the former type, neglecting the small compression of the beam, a length of the deflected beam can be equated to its original span width to give:

$$L = 2\int_0^D \frac{\sqrt{1+y'^2}}{y'}\,\mathrm{d}y. \tag{35}$$

Substituting for the slope y' from eqns (30) and (31) and using the dimensionless parameters as before, one finds:

$$2\int_{\bar{e}\bar{W}}^{\bar{\Delta}\bar{W}}\left\{1-\left[1-\frac{\pi^2\lambda^2}{2}(\bar{W}^2\bar{\Delta}'^2-\bar{Y}^2)\right]^2\right\}^{-1/2}\mathrm{d}\bar{Y}=1. \quad (36)$$

The calculation of the integral is simplified by introducing the new variable:

$$\phi=\cos^{-1}(\bar{Y}/\bar{\Delta}'\bar{W}), \quad (37)$$

which leads to the following relation in terms of an elliptical integral of the first kind:

$$E_1(\phi_0,P)-E_1(\theta_m,P)=\frac{\pi\lambda}{2} \quad (38)$$

where the phase angles and module are defined by:

$$\phi_m=\cos^{-1}\left(\frac{\bar{\Delta}}{\bar{\Delta}'}\right),\quad \phi_0=\cos^{-1}\left(\frac{\bar{e}}{\bar{\Delta}'}\right)\quad\text{and}\quad p=\frac{\pi\lambda\bar{\Delta}'}{2}. \quad (39)$$

Equation (38) can be solved numerically for $\bar{\Delta}$ and once the maximum deflection is calculated, the elastic deflection of beam can be defined as follows:

$$[2E_2(\phi_0,p)-E_1(\phi_0,p)]-[2E_2(\phi,p)-E_1(\phi,p)]=\pi\bar{\lambda}\bar{X} \quad (40)$$

where E_1 and E_2 are elliptical integrals of the first and second kinds, respectively, and the variable angle ϕ is defined by eqn (37).

The total dimensionless approach of the beam supports toward each other ($\bar{s}$) is evaluated by substituting for $\phi=\phi_m$ and $2\bar{X}=1-\bar{s}$ into eqn (40), which yields

$$\bar{s}=2-\frac{4}{\pi\lambda}[E_2(\phi_0,p)-E_2(\phi_m,p)]. \quad (41)$$

If the supports are assumed to be hinged but no relative sliding is allowed (case b), the span width will be constant and the central deflection of the beam can be calculated by direct integration of eqn (30). This operation leads to the following equation:

$$2[E_2(\phi_0,p)-E_2(\phi_m,p)]-[E_1(\phi_0,p)-E_1(\phi_m,p)]=\pi\lambda \quad (42)$$

which can be solved for the deflection $\bar{\Delta}$ as a function of the prescribed applied load.

5. DISCUSSION

The numerical solution of eqns (38) and (42) can be found using the Newton–Raphson technique. This results in the values of the maximum deflections of a centrally cracked beam as a function of the load applied. Substituting for the value of the maximum deflection into function (40) the elastica of the deflected beam is obtained. Such functions are plotted in

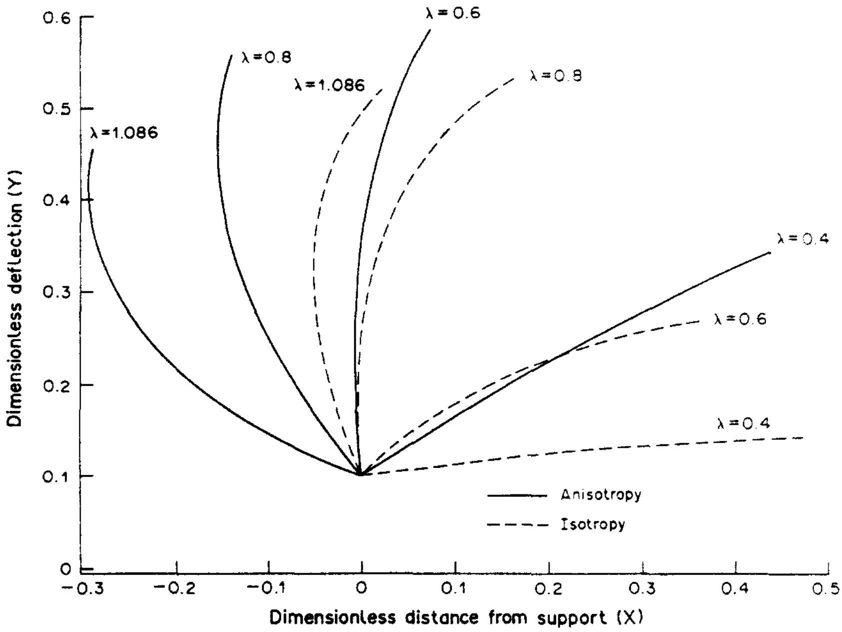

Fig. 9. Elastica of a cracked beam as a function of the dimensionless load ($\bar{a} = 0.5, \bar{e} = 0.1, w = 0.1$).

Fig. 9 for two types of isotropic ($\eta = 1$) and anisotropic ($\eta = 5.45$) composites at several loading levels, assuming $\bar{a} = 0.5$, $\bar{e} = 1$ and $\bar{W} = 0.1$. It is observed that as the load increases and the supports approach and cross over each other, the alternative tensile and compressive forces produced engender positive and negative curvatures in the buckled beam. Notably, as can be foreseen from eqn (15), the slope at the middle cross-section due to the crack flexibility increases with increasing load and deformation.

Equations (38), (41) and (42) suggest that the central deflection of the buckled beam and the approach of its moving supports to each other are generally functions of the dimensionless load factor, λ, slenderness factor, $\bar{W}$, eccentricity ratio, $\bar{e}$, crack length ratio, $\bar{a}$, flexibility of supports and material anisotropy as defined by the η-parameter. To demonstrate the influence of these parameters on the buckling behavior of the cracked column, the characteristic equations are solved for different crack length and load ratios, assuming the following arrangements:

moving roller supports (a) $\bar{W} = 0.1$, $\bar{e} = 1.0$
(b) $\bar{W} = 0.1$, $\bar{e} = 0.5$
(c) $\bar{W} = 0.25$, $\bar{e} = 0.4$
(d) $\bar{W} = 0.5$, $\bar{e} = 0.1$
fixed hinged supports (d) $\bar{W} = 0.1$, $\bar{e} = 1.0$.

In each case, two different materials were considered whose elastic constants are shown in the Appendix. The first was an isotropic material while the other was a boron–epoxy composite which has a relatively strong anisotropic behavior. In order to have an analogous basis for the comparison of the results obtained, the axial compliance factor, A_{11} was taken to be equal for both materials.

Figures 10 to 13 illustrate the results for a freely supported beam, while Fig. 14 is a representative of the fixed-span beam. In the former case the approach of supports will be a function of the dimensionless load and crack size as demonstrated in Fig. 15.

The comparative study of the pattern of deformation of different cracked beams presented in these graphs projects a clear picture of the buckling phenomenon. Generally, it is observed that the maximum slopes and deflections are monotonous functions of the load eccentricity, beam slenderness, crack length and anisotropic parameter. Provided that

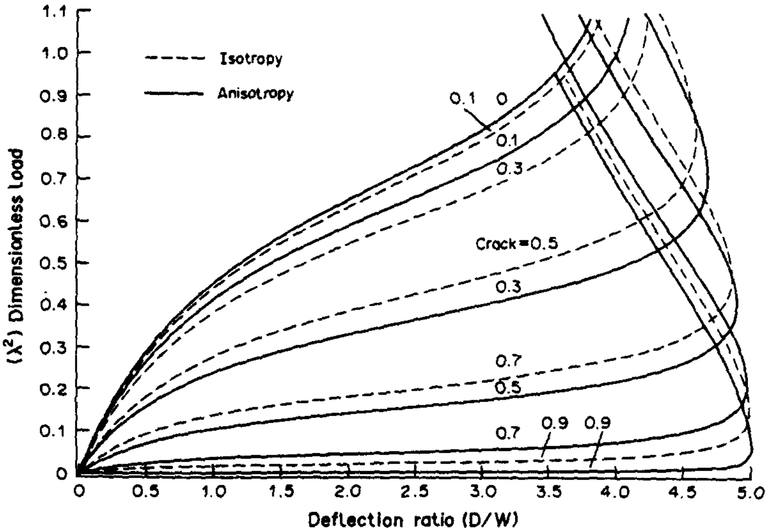

Fig. 10. Maximum deflection as a function of crack ratio and dimensionless load ($\bar{e} = 1.0$, $\bar{w} = 0.1$, hinged–roller supports).

the crack growth is prevented, theoretically infinite deflections may be obtained if supports are fixed and an endless beam is pushed eccentrically on both sides (Fig. 14). On the contrary, if the supports were free to roll and approach each other the maximum deflection will be finite (Figs 10–13).

In the present work, the transverse shear force on buckling and post-buckling of the cracked column is neglected. However, the recently published results for laminated composite materials by Kardomateas and Schmueser (1988) demonstrate that the shear deformations can significantly influence the buckling behavior of compressively-loaded structures.

In general, the additional slope of the deflected beam due to the shear force, $Q = P \sin\theta$, can be expressed as:

$$\theta_{sh} = \frac{1.2P\sin\theta}{AG_{12}} \tag{43}$$

where θ is the total slope of the beam. The error arising from neglecting this additional shearing deformation will be proportional to:

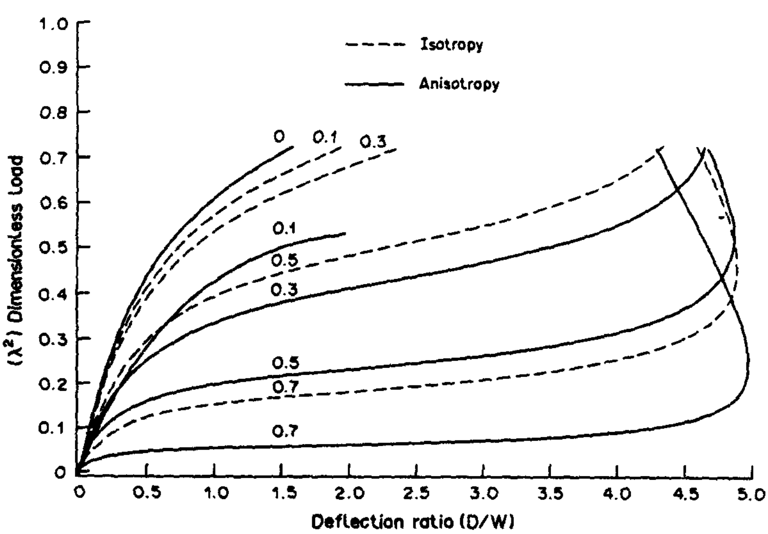

Fig. 11. Maximum deflection as a function of crack ratio and dimensionless load ($\bar{e} = 0.5$, $\bar{w} = 0.1$, hinged–roller supports).

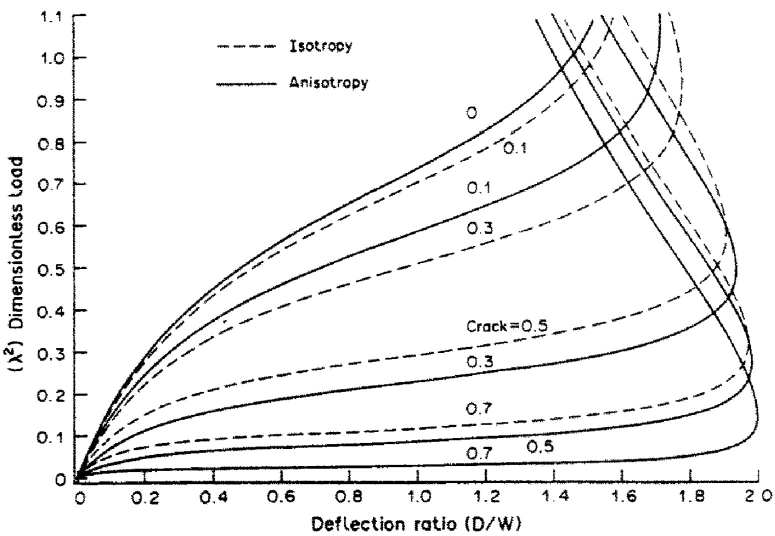

Fig. 12. Maximum deflection as a function of crack ratio and dimensionless load ($\bar{e} = 0.4$, $\bar{w} = 0.25$, hinged–roller supports).

$$\text{Error} = \lambda^2 \cdot (E_{11}/G_{12}) \cdot (w/L)^2 \cdot \sin\theta. \tag{44}$$

If the column is very thick, the error will be particularly noticeable at high load levels for anisotropic composites. This is because of the high ratios of the extensional to shear moduli of most reinforced epoxy composites (for boron–epoxy $E_{11}/G_{12} = 35$). Furthermore, the effect of shear forces is enhanced if mixed delamination phenomenon is observed (Kardomateas and Schumueser, 1988).

For uncracked systems the shear effect can be accounted for by replacing the bending rigidity $E_{11}I$ with the reduced rigidity $E_{11}I/(1.0+1.2P/AG_{12})$. However, as indicated before in Section 2, the presence of a crack in the system will further complicate the problem; since in an anisotropic cracked medium coupling of bending and shear compliances will produce a mixed mode of deformation [see eqn (6)].

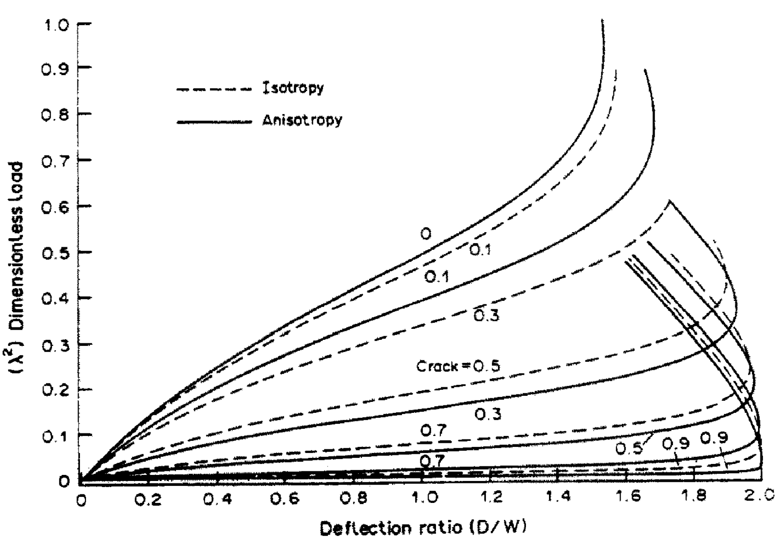

Fig. 13. Maximum deflection as a function of crack ratio and dimensionless load ($\bar{e} = 1.0$, $\bar{w} = 0.25$, hinged–roller supports).

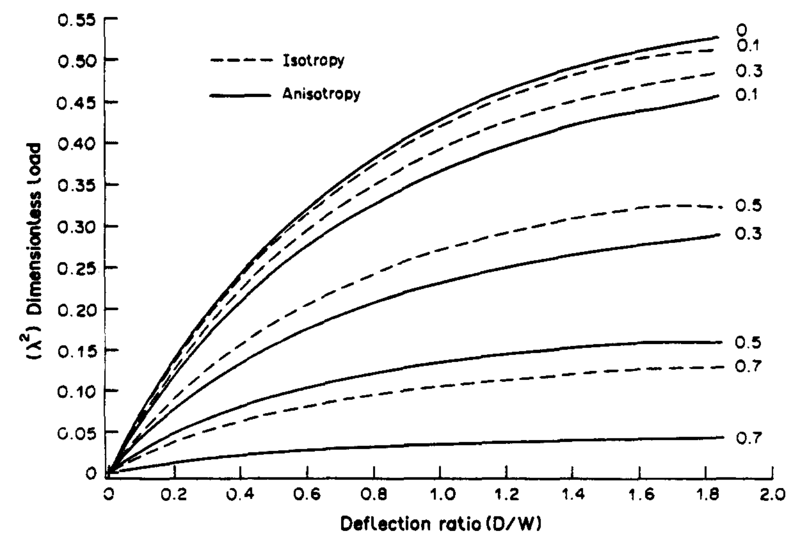

Fig. 14. Maximum deflection as a function of crack ratio and dimensionless load ($\bar{e} = 1.0$, $\bar{w} = 0.1$, hinged–fixed supports).

6. CONCLUSIONS

(1) The buckling composite cracked columns can be explained by the elliptical integral equations which similarly characterize the instability of an intact member. The specific boundary conditions at the cracked section were formulated using the well-known fracture mechanics concepts and were shown to be the very image of a flexible support with finite rotational freedom.

(2) The weakening effect of the local flexibility due to the crack drastically increases with the material anisotropy. To cite an example, the maximum deflection of the boron–epoxy composite beam with a crack length ratio of one-half at the time that the supports cross over each other ($s = 1$) is almost twice of the value calculated for an isotropic material.

(3) The theoretical load carrying capacity at the onset of buckling ($\lambda = 1$) was shown to be a square function of the crack length, linear function of anisotropic parameter and inverse function of specimen width and length [see eqn (28)].

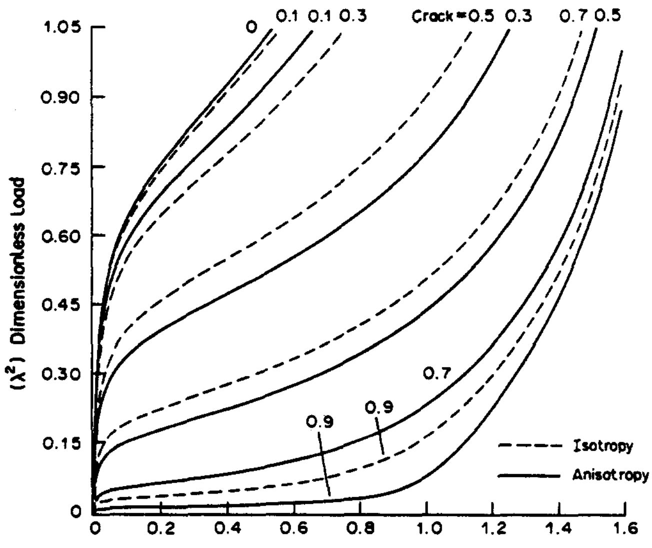

Fig. 15. Dimensionless approach as a function of load and crack length ($\bar{e} = 1$, $\bar{w} = 0.1$).

(4) Anifantis and Dimarogonas (1983) in their discussion on the buckling of isotropic cracked beams have pointed out that the effect of the compressive force on the local flexibility of beam is trivial and may be neglected. Their formulation of the problem thus indicates that the deflection equation will not directly involve the specimen width ratio. However, when the local crack flexibility appears [refer to eqns (15)–(20)], the equations also contain the specimen width. The comparison of the results shown in Figs. 10 and 13 demonstrates the extent of the error committed if the compressive loads are to be neglected. In these graphs, while the eccentricity ($e = \bar{e} * \bar{W} * L$) is kept constant, the specimens' widths ($W = \bar{W} * L$) differ. It can be seen that for all crack lengths and for both isotropic and anisotropic materials, the deflection ($\bar{D} = D * \bar{W} * L$) at any specific dimensionless load level is conspicuously larger for the wider material. It can therefore be concluded that both the bending and axial loads play important roles in the cracked beam overall flexibility.

REFERENCES

Anifantis, N. and Dimarogonas, A. (1983). Imperfection post buckling analysis of cracked columns. *Engng Fract. Mech.* **18**, 693–702.

Chondros, T. G. B. and Dimarogonas, A. (1980). Identification of cracks in welded joints of complex structures. *J. Sounds Vibr.* **69**(4), 531–538.

Delale, F., Bakirtas, I. and Erdogan, F. (1979). The problems of an inclined crack in an orthotropic strip. *J. Appl. Mech.* **46**, 90–96.

Kardomateas, G. A. and Schmueser, D. W. (1988). Buckling and postbuckling of delaminated composites under compressive loads including transverse shear effects. *J. AIAA* **26**(3), 337–343.

Kaya, A. C. and Erdogan, F. (1980). Stress intensity factors and COD in an orthotropic strip. *Int. J. Fract.* **16**, 171–190.

Liebowitz, H. L. and Claus, W. D. (1968). Failure of notched columns. *Engng Fract. Mech.* **1**, 379–383.

Liebowitz, H. L., Vondervelt, H. and Harris, D. W. (1967). Carrying capacity of notched columns. *Int. J. Solids Structures* **3**, 489–500.

Nikpour, K. (1990). Crack diagnosis in composite cylindrical shells, to be published in *J. Comp. Sci. Techn.*

Nikpour, K., Chen, Y. N. and Kardos, J. L. (1990). Fracture toughness of unidirectional short-fiber reinforced epoxy composites, to appear in *J. Comp. Sci. Tech.*

Nikpour, K. and Dimarogonas, A. (1988). Local compliance of composite cracked bodies. *Comp. Sci. Tech.* **32**, 209–223.

Okamura, H., Liu, H. W., Chu, C. S. and Liebowitz, H. L. (1969). A cracked column under compression. *Engng Fract. Mech.* **1**, 547–564.

Paipetis, N. A. and Dimarogonas, A. (1984). Post buckling behavior of transverse cracked columns. *Comput. Struct.* **18**(2), 351–356.

Papadopoulos, C. A. and Dimarogonas, A. (1987). Coupling of bending and torsional vibration of a cracked Timoshenko shaft. *Ing.-Arch.* **57**, 257–266.

Papadopoulos, C. A. and Dimarogonas, A. (1988). Stability of cracked rotors in coupled vibration mode. *Trans. ASME* **110**, 356–359.

Rice, J. R. and Levy, N. (1972). The part-through surface crack in an elastic plate. *J. Appl. Mech.* **3**, 185–194.

Sih, G. C., Paris, P. C. and Irwin, G. R. (1965). On cracks in rectilinearly anisotropic bodies. *Int. J. Fract. Mech.* **1**, 189–203.

Tada, H., Paris, P. C. and Irwin, G. R. (1973). *The Stress Analysis of Cracks Handbook*. Del Research Corporation, Hellertown, PA.

APPENDIX

The elastic constants of the material, $A_{i,j}$ are defined by equations relating stress and strain along the axes of orthotropy and for boron and glass composites used in the numerical examples are assumed to be (Delale *et al.*, 1979; Kaya and Erdogan, 1980) as follows.

	Elastic constants ($m^2\,GN^{-1}$)			
	A_{11}	A_{22}	A_{66}	A_{12}
Boron	0.00586	0.01813	0.20530	−0.00060
Glass	0.21400	0.05240	0.50000	−0.02400

When the crack extends in the direction of fiber, the anisotropic quotient in eqn (19) is calculated from eqn (10); so that for boron- and glass-epoxy composites it is equal to 5.46 and 3.60, respectively.

When the crack extension occurs in the transverse direction, A_{11} and A_{22} should be interchanged, and the anisotropic quotient has a value of 1.004 for boron and 0.435 for glass composites. These results are given for plain stress conditions and can be modified for the plain stress case, using eqns (7). For most composites, however, the difference will be insignificant.